Journal of Advances in Medicine and Medical Research

24(7): 1-15, 2017; Article no.JAMMR.37534
ISSN: 2456-8899
(Past name: British Journal of Medicine and Medical Research, Past ISSN: 2231-0614, NLM ID: 101570965)

Induction of Rat Marrow Stromal Cells by FGF2 and Insulin Activates Transcription of *runx2* Gene through *ap1* Consensus Sequence

Paweena Wongwitwichot[1] and Jasadee Kaewsrichan[2*]

[1]Department of Pharmaceutical Chemistry, Faculty of Pharmaceutical Sciences, Prince of Songkla University, Hat-Yai, Songkhla, Thailand.
[2]Department of Pharmaceutical Chemistry, Faculty of Pharmaceutical Sciences, Nanotec-PSU Center of Excellence on Drug Delivery System, Prince of Songkla University, Hat-Yai, Songkhla, Thailand.

Authors' contributions

This work was carried out in collaboration between both authors. Author PW performed the research and statistical analysis. Author JK contributed on the study's conception and design, analysis and interpretation of data and drafting the article critically for important intellectual content. Both authors read and approved the final manuscript.

Article Information

DOI: 10.9734/JAMMR/2017/37534
Editor(s):
(1) Kate S. Collison, Department of Cell Biology, King Faisal Specialist Hospital & Research Centre, Saudi Arabia.
Reviewers:
(1) Samuel Ifedioranma Ogenyi, Nnamdi Azikiwe University, Nigeria.
(2) Azza Mohamed Elamir, Fayoum University, Egypt.
(3) Takashi Ikeno, National Center of Neurology and Psychiatry, Japan.
(4) Zoulfia Allakhverdi, University of Montreal, Canada.
Complete Peer review History: http://www.sciencedomain.org/review-history/22026

Original Research Article

Received 19th October 2017
Accepted 16th November 2017
Published 23rd November 2017

ABSTRACT

Background: Signaling transductions in bone development and regeneration are complicated and relied on various growth factors functioning in an orchestrated manner. FGF2 and insulin are bone anabolic agents. Co-induction of rat marrow stromal cells (rat MSCs) by FGF2 and insulin significantly enhances *runx2* gene expression *in vitro* and bone formation *in vivo*. However, molecular mechanisms underlying these activations are scant at present.
Objective: To characterize the 5'-upstream region of *runx2* gene responsible for increasing bone formation followed by FGF2 and insulin induction.
Results: *In vitro* study showed that mRNA levels of genes including *runx2, osterix, bone morphogenetic protein 7, β-catenin, axis inhibition protein 2*, and *dickkopf-1* increasingly expressed

**Corresponding author: E-mail: jasadee.k@psu.ac.th;*
E-mail: paweena.wongwit@gmail.com;

by FGF2 plus insulin induction in compared to that of FGF2 treatment. BMP-2 and alkaline phosphatase were significantly affected by these inducers, and mineralization was improved by about 2 folds. Improvement of bone regeneration *in vivo* was apparent for inductions using FGF2 or FGF2 plus insulin, followed by BMP-2. The insulin supplement was advantageous for forming new blood vessels, although it hindered bone formation to some extent.

Conclusion: Regulation of *runx2* transcription by FGF2 and insulin seemed to mediate through the ap1 consensus locating on the 5'-upstream region of *runx2* gene. Supposedly, multiple impulses exhibit catabolic/anabolic effects on bone regeneration in rat MSCs following challenged by FGF2 and insulin.

Keywords: FGF2; insulin; runx2; maturation; bone regeneration; luciferase reporter gene assay.

1. INTRODUCTION

Marrow stromal cells (MSCs) are multipotent cells present in a scant number of several tissues, such as bone marrow, dermis, umbilical cord blood, muscle, adipose tissue, synovium and deciduous teeth. The cells are potential in differentiation to be osteoblasts, chondrocytes, myoblasts or adipocytes in response to a distinct set of cytokines [1], and may be the best cell sources for tissue engineering applications. In bone tissue engineering, the most crucial need is to promote MSCs differentiation into pre-osteoblasts by using a number of osteogenic growth factors [2,3]. Fibroblast growth factors (FGFs) are a family of growth factors involved in embryonic development and angiogenesis. Large amounts of FGFs are secreted during the processes of fracture healing [4,5], thus implicated to play important roles in bone development and repair. Among them, FGF2 (known as basic fibroblast growth factor or bFGF) is most abundant in adult tissues. Its potency on osteogenic differentiation of MSCs is either inhibitory or stimulatory depending on the presence of other cytokines [6,7] and the using doses [8,9]. An increase of initial FGF2 dosing has found to result in increased pool of pre-osteoblasts committed from MSCs population. However, such progenitors may decrease their differentiation potential when continuously challenged by FGF2 [10,11]. Nevertheless, synergism between FGF2 and bone morphogenetic protein 2 (BMP-2) on osteogenesis has been indicated only at low FGF2 doses, and a sequential induction by FGF2 and BMP-2, rather than simultaneous administration, has been mostly optimal for osteogenic inducing effect *in vitro* [10].

The consequences of insulin on bone development and osteoblast functions have been reported. For example, increased expression of insulin receptors has been demonstrated when using insulin at physiological concentration for induction, the results of which are to improve glucose uptake and utilization by the expressed cells [12]. Insulin elicits bone anabolic effect by stimulating collagen [13] and alkaline phosphatase (ALP) [14] production. Patients with type-1 diabetes mellitus (T1DM) are frequently faced with early onset osteoporosis [15], leading to increased risk of fractures [16], while bone healing after such injuries is impaired [17]. In addition, the ability on forming new bone in T1DM-animal models has been reduced, and the formed bone was deformed [18]. Interestingly, local administration of insulin has been successful for treating osteoporosis and bone fracture in diabetic patients [19]. Therefore, pathways that regulate osteogenesis and glucose homeostasis are moderately associated.

The present study is aimed to address (i), impacts of low dosing FGF2 and insulin on pre-osteoblastic commitment of rat MSCs; (ii), differentiation and mineralization potential when BMP-2 was subsequently supplied in their culture; (iii), some associated signaling pathways by using techniques of real-time PCR, protein (i.e., BMP-2) and enzyme (i.e., ALP) analyses, as well as mineralization assay; (iv), an induction scheme optimal for stimulating bone formation *in vitro* and *in vivo*; and (v), possible signaling pathways, regulatory sequences and effectors following activated by these inducers. Our goal is to obtain optimal dosing regimen of FGF2 and insulin with maximal bone regenerative capacity both in cell culture and in animals, and acquired results might be useful for clinical practice in the future.

2. MATERIALS AND METHODS

2.1 Isolation of MSCs from Rat Bone Marrow

Experiments using animals were approved by the animal care and use committee at Prince of Songkla University. Ten 8-weeks old Wistar rats

were humanely killed using guidelines adopted from IACUC [20]. Femurs and tibia were excised and ends-cut. Heparin-containing Minimum Essential Medium, alpha (α-MEM, Gibco®) was used for flushing the bone marrows and the flow-through was collected. The flow-through was gently layered over to Lymphoprep™ (Axis-shield) solution at a 1:1 volume ratio. The mixture was centrifuged at 800x*g* for 30 min. Mononuclear cells at the liquid interphase were collected, washed with phosphate buffer saline (PBS, Gibco®), and suspended in α-MEM medium supplemented with 6% fetal bovine serum (FBS, Gibco®), 1% penicillin/streptomycin (Gibco®), and 500 µg/l amphotericin B (Gibco®) to the half flow-through volume. The suspended cells were separately plated on each of four T-25 culture flasks and routinely grown to full confluence in a 5% CO_2 incubator using standard cell culture technique. The cultured medium was changed every 2-3 days. The presence of surface markers including CD13, CD29, CD44, CD73 and CD90 was investigated using flow cytometer to confirm whether these cells were of mesenchymal origin [10]. The obtained MSCs, called P_0, were ready for future use in the induction study.

2.2 Induction of P_0 Cells

The induction experiment was conducted by steps in the following. The cells at full confluence were trypsinized and re-suspended to a density of $5x10^4$ cells/ml in the growing medium previously mentioned. A 100-µl cell suspension was seeded onto a well of 6-well plates and cultured for 18 h. Then, the cultured supernatant was removed and replaced by α-MEM medium containing 2% FBS for 1 day for starvation. Inducers used included FGF2 (Merck), BMP-2 (BioVision), and insulin (Novo Nordisk Pharmaceuticals Ltd.). Each was prepared to a desired concentration regarding to our previously study [10], and preliminary results (unpublished). An induction scheme was set up as shown in Fig. 1. Briefly, the starved cells were challenged by 2.5 ng/ml FGF2, 60 ng/ml insulin or 2.5 ng/ml FGF2 plus 60 ng/ml insulin for 1 day, starved again for 2 days, and next induced by 10 ng/ml BMP-2 for 1 day. Then, the induced cells were incubated in α-MEM containing 2% FBS and 10 mmole/l β-glycerophosphate (β-GP) for another 5 days to allow mineral deposition, a so-called mineralization process. In control group, the cells were maintained in α-MEM containing 2% FBS entirely the induction phase.

2.3 Real Time Polymerase Chain Reaction (RT-PCR)

mRNA levels for genes such as *runx2*, *osterix* (*osx*), *bone morphogenetic protein 7 (bmp-7)*, *β-catenin*, *axis inhibition protein 2* (*axin2)* and *dickkopf-1 (dkk1)* were quantified using RT-PCR technique in compared to that of *gapdh* gene. Tripure® isolation reagent (Roche) was used for cell lysis, followed by performing total RNA extraction according to the manufacturer's instructions. The first cDNA strand was synthesized using Revoscript™ Reverse Transcription PreMix (Intron Biotechnology, Gyeonggi-do, Korea). Quantitative RT-PCR (qPCR) was carried out on a LightCycler® Nano Machine (Roche) using Brilliant II SYBR® Green QPCR Master Mix (Stratagene, San Diego, CA, USA). Sequences of RT-PCR primers were summarized in Table 1. A 40-thermal cycles program was set up, consisting of denaturation at 95°C for 15 sec, annealing at an optimal temperature (see Table 1) for 15 sec, and extension at 72°C for 15 sec. The threshold cycle (Ct) of the gene examined was recorded. In using similar amounts of DNA templates, results were calculated and expressed as folds-increase for the gene of interest by comparing with the Ct of *gapdh* gene.

2.4 Expression of BMP-2 Protein

The expressed BMP-2 was determined in cell supernatant using Quantikine® BMP-2 ELISA Kit (R&D System, Minneapolis, MN, USA). A clear supernatant was obtained by centrifugation at 12000x*g* for 10 min. Its volume of 100-µl was added to a well of BMP-2 antibody pre-coated microplate and removed after incubation at room temperature for 2 h. The well was washed 4 times with washing buffer, followed by the addition of horseradish peroxidase-conjugated BMP-2 antibody and the incubation at room temperature for 2 h. The antibody solution was then withdrawn and the well was completely washed with washing buffer. Next, tetramethylbenzidine substrate was added, incubated for 30 min in the dark, followed by adding the stop solution to terminate the reaction. The OD_{450} was measured within 30 min. The BMP-2 standard curve was prepared according to the manufacturer's recommendations. The amount of cellular protein in the corresponding well was quantified using Pierce® BCA protein assay kit (Pierce, Rockford, IL, USA). The amount of BMP-2 was calculated by comparing with the standard curve and normalized by the assayed protein concentration.

2.5 Assay of ALP Activity

ALP is an early marker of osteogenesis, normally presenting on the cell membranes of osteoblasts [21]. A colorimetric assay format has been used by many studies [22,23] for measuring cellular ALP activity, including this research. In detail, lysis buffer pH 7.0 (50 mmole/l Tris, 1% Triton x-100, and 150 mmole/l NaCl) was added onto cell monolayer in a well following cultured medium was removed. By incubation at room temperature for further 30 min, cell lysate was obtained. A 25-µl cell lysate was added to a tube containing 75 µl of ALP substrate buffer (10 mmole/l p-nitrophenylphosphate, 10 mmole/l $MgCl_2$ mole/l Tris-HCl, ph 9.0). After thoroughly mixed and incubated at 37°C for 30 min, a 10-µl stop solution (2 mole/l NaOH) was added, and the OD_{405} was measured within 30 min. Data were normalized by the amounts of cellular protein in the corresponding wells and reported as relative ALP activity.

2.6 Assay of Mineralization

Mineralization was assessed after the induced cells were grown in the medium containing β-GP for 5 days. Briefly, the cells in a well of 6-well plates were washed with PBS, fixed with para-formaldehyde (4% in PBS) for 15 min, and then washed several times with distilled water. These cells were stained by using 2% alizarin red S (pH 4.2) and incubated at room temperature for 20 min. The excess dye was removed, while the cells were completely washed with distilled water and allowed for air dry. Photography was carried out using the Cell P Software-controlling camera (Olympus). A mixture of 20% methanol and 10% acetic acid was used to dissolve dye that stained the cells. By incubation for 20 min, the dissolved dye was collected and the OD_{450} was measured. Data were normalized by the OD_{570} obtained from MTT assay [10] for the corresponding wells and reported as relative mineralization.

2.7 Seeding Cells on Scaffolds and Induction

Scaffolds were prepared in our laboratory according to the previous study [24]. The P_0 cells with an identical number to that of the *in vitro* induction experiment were gradually seeded onto a sterile scaffold placed on a well of 6-well plates. The seeded scaffold was incubated in a 5% CO_2 incubator for 1 h to allow cell attachment. Similarly, the induction scheme of Fig. 1 was applied for the cells seeded on scaffolds, but the last incubation with β-GP was excluded. After the induction was completed, each of the scaffolds was subcutaneously implanted in a rat. Scaffolds without cells and cell-seeded scaffolds without induction were used as control groups.

2.8 Animals, Surgical Procedure and Implantation

Five male Wistar rats (8-weeks old, weight 220-250 g) were anesthetized by intramuscular injection of 100 µl per 100 g body weight of a mixture containing a 1:1 volume ratio of xylazine (25 mg/ml; Thai Nakorn Patana, Nonthaburi, Thailand) and Zoletil® 100 (12.5 mg/ml; Virbac Pty Limited, Australia). The lumbar area of a rat was disinfected and shaved, and five separate pockets with 6 mm wide were subcutaneously created. Each pocket was inserted with a test implant. Five different implant samples were investigated, including cell-free scaffold, cell-seeded scaffold without induction (2%FBS), cell-seeded scaffold with FGF2/BMP-2 induction, cell-seeded scaffold with insulin/BMP-2 induction cell-seeded scaffold with FGF2+insulin/BMP-2 induction. The wounds were closed by taking the 4-0 silk sutures, and a topical antimicrobial cream was applied on the operated lesions for 1 week.

2.9 Histological Analysis

The animals were sacrificed after 8 weeks of implantation. The implants were excised, fixed in 10% v/v formaldehyde in PBS for 24 h, and decalcified in 1 mole/l HCl saturated with EDTA for 2 days. The decalcified sample was paraffin embedded and sectioned to a 5-µm thick layer. The section was stained with hematoxylin/eosin (H&E) or alizarin red S. The Cell P Software-controlling light microscope (Olympus) was used to photograph, and data of three different levels for each section were delicately analyzed.

2.10 Construction of Luciferase-reporter Plasmids

A set of plasmids containing genes of firefly (*luc*) or *Renilla* luciferase (*Rluc*) was purchased from Promega (Madison, WI, USA). The 5'-upstream region of *runx2* gene (Accession no. NC_005108) between −1526 and −73 base pairs (bps) were amplified by PCR technique using two sets of primer pairs (see Table 2). A 50-µl PCR mixture was prepared to contain 25 mmole/l KCl, 25 mmole/l NaCl, 35 mmole/l Tris-HCl pH 9.0, 1.5 mmole/l $MgCl_2$, 0.5 mmole/l dNTPs,

0.6 µmole/l of each primer, 2.5 U of Taq DNA polymerase (Intron Biotechnology) and 100 ng of DNA template. PCR reaction was performed on G-Strom GS00482 thermal cycler (Gene Technology LTD, England). PCR product from each reaction was cloned into pGL3-reporter vector obtaining two recombinant reporter plasmids, namely pGL3-*runx2*-N and pGL3-*runx2*-F (see Fig. 2). The cloned DNA fragment was annotated by using TFSEARCH software, according to the previous study [25]. Two possible consensuses were determined to associate with osteogenesis, such as activator protein 1 (*ap1*) and sex-determining region Y (*sry*/*sox*) sites. This possibility was proved by cloning double-stranded DNA fragment containing five-times repeat of *ap1* or *sry/sox* consensus sequence (commercially synthesized by Bio Basic Canada Inc., Canada; see Table 2) into pGL3-reporter vector. Other two recombinant reporter plasmids were acquired, namely pGL3-5x(*ap1*) and pGL3-5x(*sry*), respectively. These four reporter constructs were separately used to transfect the P_0 cells.

2.11 Co-transfection of the P_0 Cells

A reporter construct was co-transfected with the *Rluc* control plasmid (pRL-SV40) into the P_0 cells using an optimal weight ratio of the DNAs, according to our preliminary results (unpublished). In brief, DNA mixture containing 0.4 µg of a reporter plasmid and 8 ng of pRL-SV40 was prepared, added in a tube containing 2.4 µl of FuGENE® 6 Transfection Reagent (Roche). After thoroughly mixed and incubated at room temperature for 15 min, 100 µl of serum-free α-MEM medium were inoculated. The P_0 cells of 70% confluence grown in a well of 24-wells plates were incubated with the DNA mixture for 4 h before removal. The transfected cells were starved in 2% FBS supplemented α-MEM for 1 day, induced with 2.5 ng/ml FGF2, 60 ng/ml insulin or 2.5 ng/ml FGF2 plus 60 ng/ml insulin for 1 day, maintained in the starving medium for another 1 day, and followed by assay of dual luciferase activity. For the control, the transfected cells were entirely cultured in the starving medium for 3 days.

Table 1. Sequences of primers for RT-PCR

Gene [reference gene]	Sequence (5'→3')		Expected product size (bp)	Annealing temperature (°C)
gapdh [NM_017008]	F	ACC ACA GTC CAT GCC ATC AC	179	59
	R	ACA CGG AAG GCC ATG CCA GTG		
runx2 [NM_001278483]	F	ACA ACC ACA GAA CCA CAA G	106	55
	R	TCT CGG TGG CTG GTA GTG A		
osx [NM_001037632]	F	AAC TGG CTT TTC TGT GGC A	237	57
	R	CGG CTG ATT GGC TTC TTC T		
bmp-7 [XM_342591]	F	GAC AGA TTA CAG ACT CCC ACA	215	54
	R	GTT GAT GAA GTG AAC CAG TGT		
axin2 [NM_024355]	F	ACG AGT CAG CCG GCA CCA TC	165	57
	R	TGG GGC TTT GAC ACC TCG GC		
dkk1 [NM_001106350]	F	GCT GCC CCG GGA ATT ACT GCA	422	56
	R	GTG TCT CTG GCA GGT GTG GAG C		
β-catenin [NM_053357]	F	CGC CTT TGC GGG AAC AGG GT	121	57
	R	CGG ACG CCC TCC ACG AAC TG		

Table 2. Sequences of primers for PCR amplification of the5'-upstream sequence of *runx2* gene with 5'-*Kpn*I and 3'-*Nhe*I restriction sites, and the 5x(*ap1*) and 5x(*sry*) sequences with 5'-*Bgl*II and 3'-*Kpn*I restriction sites. Restriction sites were underlined

Name of primers or sequences	Sequence (5'→3')		T_m (°C)	Expected product size (bp)
runx2-N	F	CGC GGT ACC TTA CAG TCA ATC CCG GCA AGG	64	723
	R	GCC GCT AGC CAT GTG GTT TGT GAC CTC ACA G		
runx2-F	F	CGC GGT ACC AGG AAA TTG GTC TGC TCG CCT	58	896
	R	GCC GCT AGC GTG GGT CAC ATC TTG GGA TTG		
5x(*ap1*)	GAT CTC TGA CTC ATC TGA CTC ATC TGA CTC ATC TGA CTC ATC TGA CTC ATG GTA C			
5x(*sry*)	GAT CTT TTG TTT TTT GTT TTT TGT TTT TTG TTT TTT GTT TGG TAC			

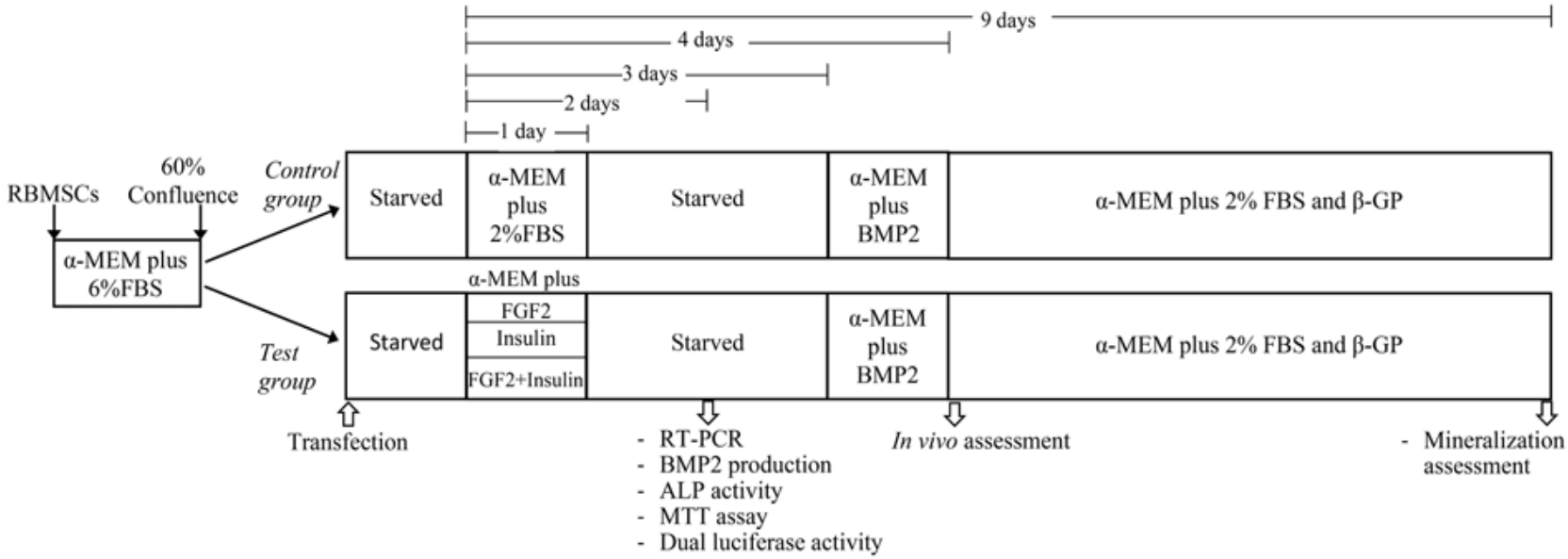

Fig. 1. An induction scheme for rat MSCs. FGF2 (2.5 ng/ml), BMP-2 (10 ng/ml), and insulin (60 ng/ml) were utilized as inducers. The cells were starved in α-MEM supplemented with 2% FBS for 1 day before induction. There were three phases for induction, i.e., the first phase was of using FGF2, insulin, or FGF2 plus insulin for 1 day, the second phase was of using BMP-2 for 1 day, and the third phase was of using 10 mmole/l β-GP for 5 days. Changes in mRNA expression were monitored by RT-PCR technique. The level of BMP-2 protein was quantified by ELISA technique, and ALP activity was determined by a colorimetric assay. Cell viability was assessed by MTT method. The degree of mineralization was assayed by measuring the OD_{450} of alizarin red S dye following dissolved from the stained cells

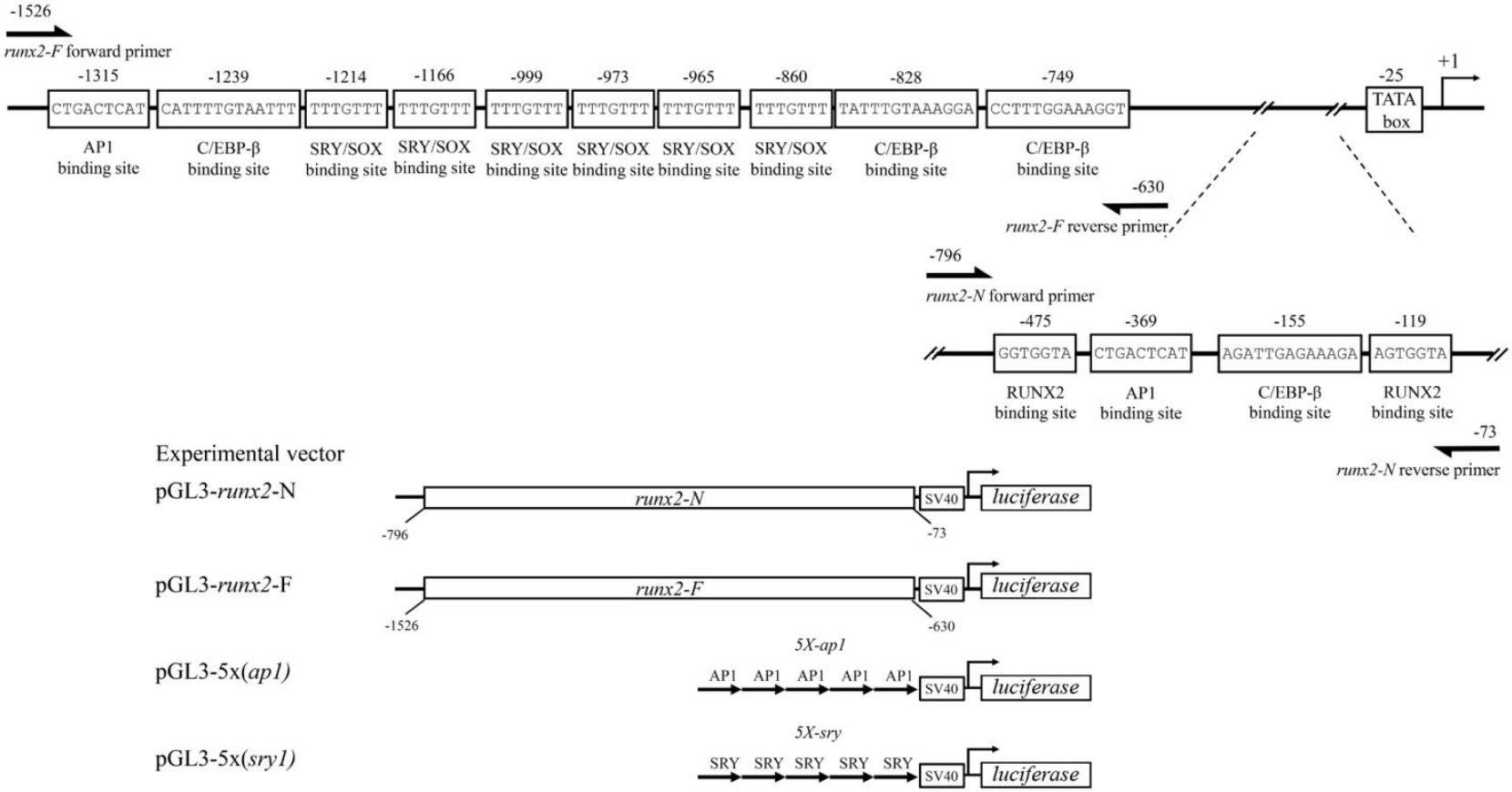

Fig. 2. Consensus sequences at the 5'-upstream of *runx*2 gene, annotated by using TFSEARCH, and maps of recombinant reporter plasmids used for transfection and dual luciferase activity assay

2.12 Assay of Dual Luciferase Activity

The dual luciferase activity was quantified by using Dual-Luciferase® reporter assay kit (Promega, Madison, WI, USA) and GloMax® 20/20 Luminometer (Promega). The *luc* and *Rluc* signals were rationed, normalized by the amount of cellular protein in the corresponding wells, and expressed as relative light units (RLUs).

2.13 Statistical Analysis

Data were reported as means ± standard deviation (SD). Student's *t*-test was used for comparing two small sets of data, while ANOVA was used when large data groups were compared. *P<0.05* was considered statistically significant. Inter-observer reliability of the histological score evaluation was assessed by determining the limits of agreement using Bland and Altman plots. SPSS software 16 was used for statistical analysis. The limits of agreement for the histological scoring was -0.6 ± 1.3 (range of score 0-24).

3. RESULTS

3.1 mRNA Levels of Genes Associating Osteogenesis

After the P_0 cells were induced by FGF2, insulin, or FGF2 and insulin for 1 day, the mRNA transcripts of *runx2*, *osx*, *bmp-7*, *β-catenin*, *axin2*, and *dkk1* genes were measured using RT-PCR technique. In Fig. 3, all of these genes were down-regulated by FGF2. Insulin had stimulatory effect on *bmp-7* gene, whereas other genes were not affected. Interestingly, these genes were significantly up-regulated by FGF2 and insulin.

3.2 Production of BMP-2 and ALP

The amounts of BMP-2 in cultured supernatants were quantified using ELISA technique. ALP activity was colorimetrically determined. These assays were done following the P_0 cells were induced by FGF2, insulin, or FGF2 and insulin for 1 day. In Fig. 4, increased BMP-2 production was observed by all of the used inducers. Insulin showed the highest inducing effect. Instead, the produced BMP-2 level was comparable for the cells induced by FGF2 or FGF2 and insulin. In Table 3, improved ALP activity was assigned for the cells treated with either FGF2 or insulin. In contrast, lowered ALP activity was found for the cells induced with FGF2 plus insulin.

3.3 Mineralization

Regarding the mineralization assay, it was carried out to differentiate the ability of the induced cells to deposit minerals when forming new bone. In Table 3, approximately 2-folds increment of the mineralization was demonstrated for the cells induced by FGF2, insulin, and FGF2 plus insulin.

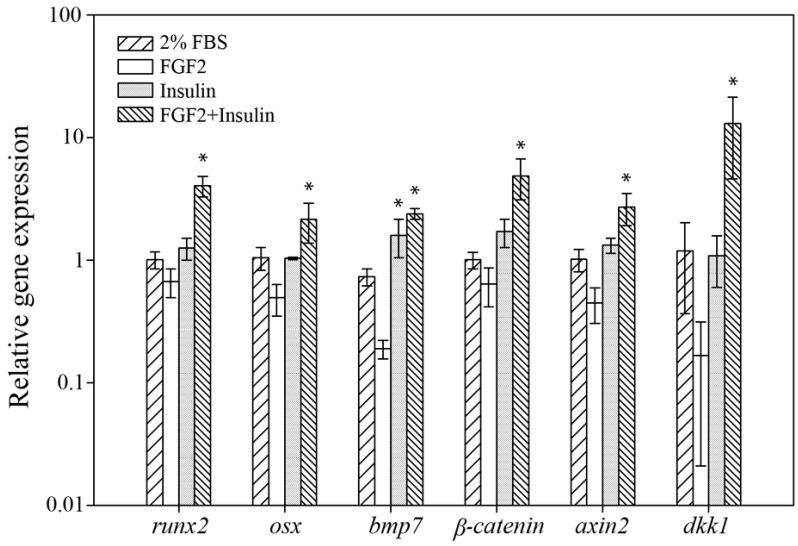

Fig. 3. mRNA levels as determined by RT-PCR technique. Relative expression (folds increase) of *runx2*, *osx*, *bmp-7*, *β-catenin*, *axin2*, and *dkk1* genes on day 1 post-induction by FGF2, insulin, or FGF2 plus insulin, *indicates significant differences (*P*<0.05) as calculated by Student's *t*-test

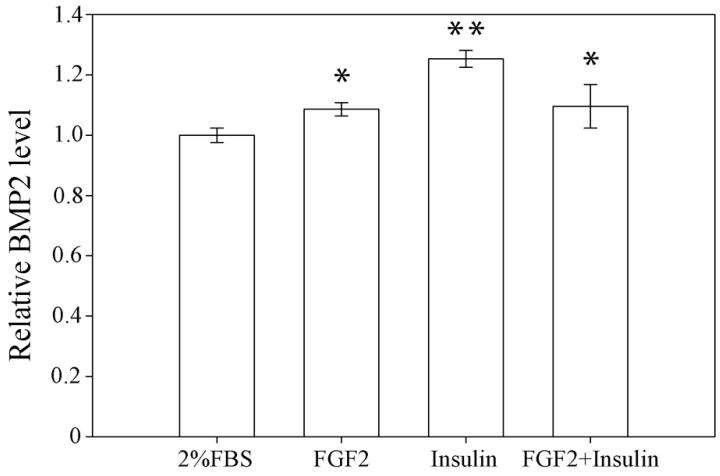

Fig. 4. Production of BMP-2 by the P_0 cells after induced by FGF2, insulin, or FGF2 plus insulin for 1 day. * and **indicate significant differences of $p<0.05$ and $p<0.01$, respectively as calculated by one-way ANOVA

Table 3. Relative ALP activity and mineralization of the MSCs challenged by different inducer(s)

Inducer(s)	Relative ALP activity (SD)	Relative mineralization (SD)
2% FBS	1.00 (0.06)	1.00 (0.03)
FGF2	1.11 (0.01)*	1.90 (0.09)*
Insulin	1.17 (0.02)*	2.01 (0.15)*
FGF2+Insulin	0.95 (0.01)*	1.92 (0.05)*

**indicates significant differences (P< 0.05) as calculated by Student's t-test*

3.4 Bone Regeneration Capacity

The effects of FGF2, insulin, and FGF2 plus insulin on bone regeneration were additionally investigated *in vivo* using a rat model. The P_0 cells were seeded onto scaffolds and subsequently induced by conditions previously used in the *in vitro* induction experiment (see Fig. 1). The cell-seeded scaffolds were subcutaneously implanted in rats (Fig. 5A), and histological analysis was performed after 8 weeks of implantation. In Fig. 5B, less bone formation was determined for the loaded cells induced by insulin/BMP-2 (Fig. 5B-g, h). Increased amounts of newly formed bone were found for the cells treated by FGF2/BMP-2 (Fig. 5B-e, f) or FGF2+insulin/BMP-2 (Fig. 5B-i, j). Although FGF2 alone exhibited greater osteoinductive activity than that of FGF2+insulin, forming of new small blood vessels within the scaffold material was detected only for the co-inducers. Bone forming area was not detected on the scaffolds lacking cells and those containing un-induced cells (2%FBS).

3.5 Assay of Dual Luciferase Activity

Since *in vitro runx2* transcription and *in vivo* bone formation and angiogenesis of the P_0 cells were encouraged by FGF2 and insulin induction (Figs. 3 and 5), it was curious to examine where and what regulatory elements in the 5'-upstream region of *runx2* gene responsible for these inductive effects. Experiments regarding luciferase reporter gene assay were consequently carried out, focusing on the 5'-upstream sequence between −1526 and −73 bps. Two recombinant reporter plasmids, namely pGL3-*runx2*-N and pGL3-*runx2*-F were successfully constructed and transfected into the P_0 cells. The transfected cells were induced by FGF2, insulin, or FGF2 and insulin for 1 day, followed by the measurement of dual luciferase activity. In Fig. 6, the RLUs of pGL3-*runx2*-N transfected cells were reduced by FGF2 induction. Instead, the signals were enhanced by 4 and 3.5 folds when insulin and FGF2 plus insulin were of the inducers. Less improvement of the RLUs was revealed by pGL3-*runx2*-F transfected cells, concerning about 1.5-, 1.8- and 2.5-folds increase for FGF2, insulin, and FGF2 plus insulin induction, respectively. In analysis of the cloned DNA fragments by using TFSEARCH software [25], two consensus sequences possibly associating bone repair processes were annotated. These were *ap1* (CTGACTCAT) and *sry/sox* (TTTGTTT). Five times repeated sequence of each was synthesized and cloned

into the pGL3-reporter plasmid to certify protein binding ability. Another two recombinant reporter plasmids, called pGL3-5x(*ap1*) and pGL3-5x(*sry*), were obtained (see Table 2 and Fig. 2). Following transfection into the P_0 cells and induction by the above inducers, results showed that the RLUs of pGL3-5x(*ap1*) transfected cells were unaffected by insulin and slightly increased by FGF2 (1.2 folds). Instead, the signals were enhanced by FGF2 plus insulin (2 folds). For pGL3-5x(*sry*) transfected cells, the RLUs were not affected by FGF2 plus insulin, slightly increased by insulin (1.2 folds), but decreased by FGF2 (Fig. 6).

4. DISCUSSION

Runx2 is a major transcription factor associating the commitment of MSCs towards osteogenesis, rather than chondrogenesis, adipogenesis, and myogenesis [2], and works in collaboration with a number of cytokines and transcription factors to complete its responsible roles [26,27]. For the present study in which rat MSCs culture was used, the transcription of *runx2* gene was up-regulated as induced by FGF2 and insulin (Fig. 3). Increased expression of *osx*, *bmp7*, *β-catenin*, *axin2*, and *dkk1* genes were clearly observed in compared to that using only FGF2 or insulin. However, the productions of BMP-2 and ALP by the induced cells were in comparable amounts to that of the un-induced cells. Instead, mineralization was considerably achieved by the induced cells (Table 3). The *in vitro* induction scheme (see Fig. 1) was subsequently applied for the MSCs seeded on scaffolds, and the scaffolds were subcutaneously implanted in rats. After 8 weeks, new bone was distinctly observed

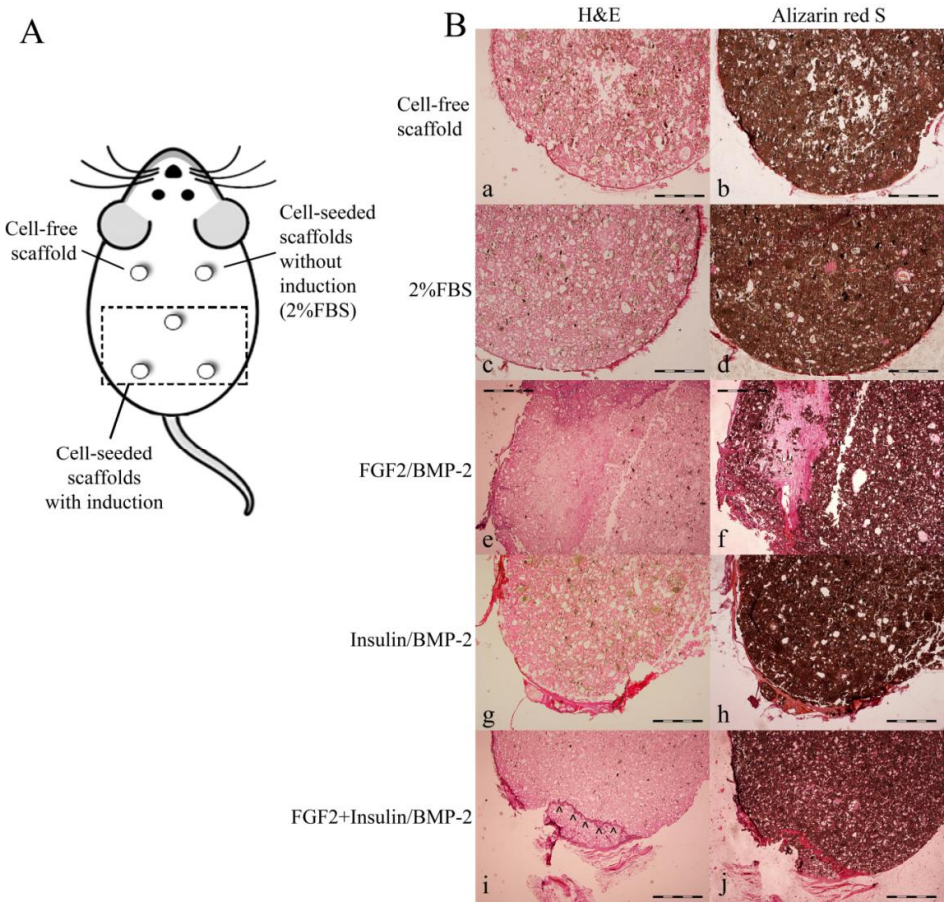

Fig. 5. A, Implantation sites on the lumbar of a rat. Five groups of scaffold samples were indicated: cell-free scaffold, cell-seeded scaffold without induction (2%FBS), and 3 groups of cell-seeded scaffold with induction (including FGF2/BMP-2, insulin/BMP-2 and FGF2+insulin/BMP-2); B, The representative histological sections stained by H&E and alizarin red. Symbols: arrow heads, small blood vessel; bar scale, 500 μm in length

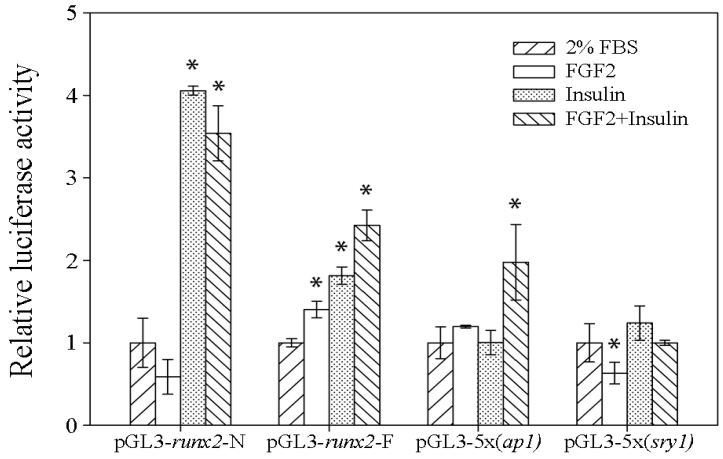

Fig. 6. Relative luciferase activity. The MSCs were transfected by pGL3-*runx*2-N, pGL3-*runx*2-F, pGL3-5x(*ap1*), or pGL3-5x(*sry*) (see also Fig. 2), and induced by FGF2, insulin, or FGF2 plus insulin for 1 day. The relative luciferase activity was measured 1 day post-induction. *indicates significant difference (*P*<0.05) as calculated by Student's *t*-test

on the scaffolds as challenged by FGF2/BMP-2 or FGF2+insulin/BMP-2 (Fig. 5B-e, f and Fig. 5B-i, j). Interestingly, new small blood vessel was solely apparent on the FGF2+insulin pretreated implants (Fig. 5B-i, j). FGF2 might take part in stimulation of forming new bone, because it presents both osteoinductive and mitogenic effects [7,11]. Regarding to new blood vessels, this might be due to an additive effect of insulin on inducing VEGF expression that subsequently supports angiogenesis [28]. In addition, there were defects in the scaffold's structure. The presence of voids might assist cell movement and infiltration, beneficial for the cells to form new bone. Therefore, this FGF2+insulin mixture might provide optimal impulses to direct the commitment of MSCs towards osteogenesis, and *runx2*-dependent signaling pathway [27] or BMP2-independent signaling transduction [29] or both were supposed as mechanisms associating their induction.

The canonical Wnt pathway is critically implicated in bone biology and pathology, and β-Catenin is one of downstream signaling molecules of this pathway [30]. Deficiency of β-catenin in osteoblasts can cause impaired maturation and mineralization [31,32], whereas increased production of Axin2 promotes β-catenin degradation [32]. In T1DM patients, the cellular β-catenin levels are reduced, leading to decreased bone density and osteopenia [33]. *Runx2* and Osx are osteogenic transcription factors regulated by the Wnt pathway [34]. DKK1 is a Wnt antagonist [35]. Inactivation of the Wnt pathway by increased expression of DKK1 and Axin2 has been reported [36]. In this research, increased transcriptions of *dkk1* and *axin2* genes were demonstrated by FGF2 and insulin induction. However, maturation and mineralization of the MSCs were not affected (Table 3). It was supposed that there were multiple signaling pathways downstream of the FGF2/insulin induction associating bone repair processes.

Although a central role of *runx2* in directing bone regeneration has been suggested by a series of researches [37,38], understanding of how it is regulated to express is somewhat limited. In this study, luciferase reporter assay was carried out to identify possible regulatory elements of *runx2* gene in rat MSCs culture, concerning the non-coding sequence ranging between −1526 and −73 bps. Following FGF2/insulin induction, the RLUs of the cells containing a (−796) – (−73) bps DNA fragment were significantly increased in compared to those harboring a (−749) – (−1526) bps fragment (Fig. 6). Two Cbfa1-binding sites (−119 and −475), one C/EBP-β-binding site (−155), and one AP1-binding site (−369) were annotated on the former DNA fragment using TFSEARCH software [25]. In addition, three binding sites of C/EBP-β (−749, −828, and −1239), six binding sites of SRY/SOX (−860, −965, −973, −999, −1166, and −1214), and one binding site of AP1 (−1315) were existing on the late DNA fragment. These were in accord with the previous studies [39,40]. Interestingly, significant reduction of the RLUs was notified by the cells containing DNA fragments with C/EBP-

β and SRY/SOX binding sites. Nonetheless, the SRY/SOX binding sites were presumed to majorly impede the signals, because they were present in duplicate numbers compared to the sites for C/EBP-β binding. To verify this assumption, the cells receiving an oligonucleotide of 5-times repeated SRY/SOX sequence were induced by FGF2 and insulin and measured for the RLUs. The responsible signals were drastically reduced, suggesting that the SRY/SOX consensuses were binding sites for antagonistic factors downstream of FGF2/insulin induction. Additionally, the significance of the Cbfa1 consensuses as binding sites for existing effecters following induced by FGF2 and insulin was investigated. Since the AP1 consensus (TGAG/CTCA) was annotated on both the (−796) – (−73) bps and the (−749) – (−1526) DNA fragments, its association on effecter binding was also examined. The RLUs of the cells acquiring the former DNA fragment were strongly improved in compared to those having the late DNA fragment. Regarding to the cells containing a 5-times repeated sequence of AP1, the responsible signals were insignificantly different from that of harboring the late DNA fragment. The results supported an idea that the *ap1* consensus might be meaningful in binding to an effecter, in particular AP1 protein, to activate *runx2* transcription as challenged by FGF2 and insulin. Although the existence of AP1 protein by FGF2/insulin induction was not proved in this study by using immunoprecipitation technique, its involvement in osteoblastic differentiation by interacting with *runx2* has been reported [2]. Moreover, the sites for AP1 binding might function synergistically with the Cbfa1-binding sites to encourage *runx2* transcription, since the RLUs of the cells containing both consensuses (pGL3-*runx2*-N in Fig. 2) were extremely enhanced, compared to that having only the AP1 sequence. Previous studies have suggested the Cbfa1-binding site as a known target for defined effectors of BMP-2 and TGF-β signaling pathways [41], responsible for feedback inhibition mechanisms of *runx2*-induced osteogenesis [42].

5. CONCLUSION

The MSCs were speedily committed to be osteoblastic progenitors by FGF2 and insulin induction. This was indicated by the increase of *runx2*, *osx*, *bmp7* and *β-catenin* gene transcription and mineralization. The *ap1* consensus on the 5'-upstream region of *runx2* gene was implicated in the induction, leading to improved osteogenesis. FGFs-, BMPs- and the canonical Wnt-signaling pathways seemed to take part in the MSCs maturation that mediated *runx2* transcription factor. The integration of multiple inputs was suggested to regulate *runx2* transcription by mechanisms as proposed in Fig. 7. Regarding the 5'-upstream sequence of *runx2*

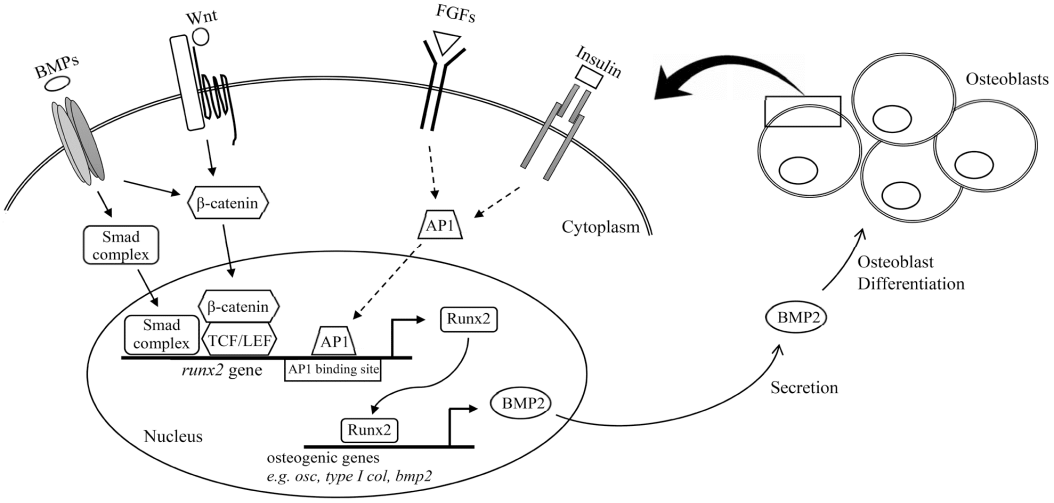

Fig. 7. Signal transductions proposed to be existent in rat MSCs after induced by FGF2 plus insulin. The *ap1* consensus on the 5'-upstream region of *runx2* gene was implicated in the induction, leading to increased *runx2*, *osx*, *bmp7* and *β-catenin* gene transcription and mineralization. Regarding the MSCs maturation, crosstalk among FGFs-, BMPs-, and the canonical Wnt-signaling pathways would be possible and might be mediated through *runx2* transcription factor

gene for rats and humans, there is about 75.5% identity according to data of pair-wise alignment (not shown). Consequently, these results would be useful in preparing pre-osteoblasts of human MSCs for therapeutic applications of fracture healing and bone tissue regeneration in the future.

CONSENT

It is not applicable.

ETHICAL APPROVAL

All authors hereby declare that "Principles of laboratory animal care" (NIH publication No. 85-23, revised 1985) were followed, as well as specific national laws where applicable. All experiments have been examined and approved by the appropriate ethics committee.

ACKNOWLEDGEMENTS

This work was supported by the Nanotechnology Center (NANOTEC), NSTDA, Ministry of Science and Technology, Thailand, through its program of Center of Excellence Network on Drug Delivery System at Faculty of Pharmaceutical Sciences, Prince of Songkla University, and the Graduate School at Prince of Songkla University.

COMPETING INTERESTS

Authors have declared that no competing interests exist.

REFERENCES

1. Pittenger MF, Mackay AM, Beck SC, Jaiswal RK, Douglas R, Mosca JD, et al. Multilineage potential of adult human mesenchymal stem cells. Science. 1999; 284(5411):143-7.
2. Deng ZL, Sharff KA, Tang N, Song WX, Luo J, Luo X, et al. Regulation of osteogenic differentiation during skeletal development. Front Biosci. 2008;13(1): 2001-21.
3. Huang Z, Nelson ER, Smith RL, Goodman SB. The sequential expression profiles of growth factors from osteroprogenitors to osteoblasts *in vitro*. Tissue Eng. 2007; 13(9):2311-20.
4. Ornitz DM, Itoh N. Fibroblast growth factors. Genome Biol. 2001;2(3):1-12.
5. Bolander ME. Regulation of fracture repair by growth factors. Proc Soc Exp Biol Med. 1992;200(2):165-70.
6. Biver E, Soubrier A-S, Thouverey C, Cortet B, Broux O, Caverzasio J, et al. Fibroblast growth factor 2 inhibits up-regulation of bone morphogenic proteins and their receptors during osteoblastic differentiation of human mesenchymal stem cells. Biochem Biophys Res Commun. 2012; 427(4):737-42.
7. Kizhner T, Ben-David D, Rom E, Yayon A, Livne E. Effects of FGF2 and FGF9 on osteogenic differentiation of bone marrow-derived progenitors. *In vitro* Cell Dev Biol Anim. 2011;47(4):294-301.
8. Berrada S, Lefebvre F, Harmand M-F. The effect of recombinant human basic fibroblast growth factor rhFGF-2 on human osteoblast in growth and phenotype expression. *In vitro* Cell Dev Biol Anim. 1995;31(9):698-702.
9. Ou G, Charles L, Matton S, Rodner C, Hurley M, Kuhn L, et al. Fibroblast growth factor-2 stimulates the proliferation of mesenchyme-derived progenitor cells from aging mouse and human bone. J Gerontol A Biol Sci Med Sci. 2010;65(10):1051-9.
10. Kaewsrichan J, Wongwitwichot P, Chandarajoti K, Chua K, Ruszymah B. Sequential induction of marrow stromal cells by FGF2 and BMP2 improves their growth and differentiation potential *in vivo*. Arch Oral Biol. 2011;56(1):90-101.
11. Fakhry A, Ratisoontorn C, Vedhachalam C, Salhab I, Koyama E, Leboy P, et al. Effects of FGF-2/-9 in calvarial bone cell cultures: differentiation stage-dependent mitogenic effect, inverse regulation of BMP-2 and noggin, and enhancement of osteogenic potential. Bone. 2005;36(2):254-66.
12. Ituarte EA, Halstead LR, Iida-Klein A, Ituarte HG, Hahn TJ. Glucose transport system in UMR-106-01 osteoblastic osteosarcoma cells: Regulation by insulin. Calcif Tissue Int. 1989;45(1):27-33.
13. Kream BE, Smith MD, Canalis E, Raisz LG. Characterization of the Effect of Insulin on Collagen Synthesis in Fetal Rat Bone. Endocrinology. 1985;116(1):296-302.
14. Pun K, Lau P, Ho P. The characterization, regulation, and function of insulin receptors on osteoblast-like clonal osteosarcoma cell line. J Bone Miner Res. 1989;4(6):853-62.
15. Kemink S, Hermus A, Swinkels L, Lutterman J, Smals A. Osteopenia in insulin-dependent diabetes mellitus;

prevalence and aspects of pathophysiology. J Endocrinol Invest. 2000;23(5):295-303.

16. Janghorbani M, Feskanich D, Willett WC, Hu F. Prospective study of diabetes and risk of hip fracture the nurses' health study. Diabetes Care. 2006;29(7):1573-8.
17. Loder RT. The influence of diabetes mellitus on the healing of closed fractures. Clin Orthop Relat Res. 1988;232:210-6.
18. Verhaeghe J, Suiker A, Visser W, Van Herck E, Van Bree R, Bouillon R. The effects of systemic insulin, insulin-like growth factor-I and growth hormone on bone growth and turnover in spontaneously diabetic BB rats. J Endocrinol. 1992;134(3):485-92.
19. Gandhi A, Beam HA, O'Connor JP, Parsons JR, Lin SS. The effects of local insulin delivery on diabetic fracture healing. Bone. 2005;37(4):482-90.
20. Leary S, Underwood W, Anthony R, Cartner S, Corey D, Grandin T, et al. AVMA guidelines for the euthanasia of animals; 2013.
21. Tsai MT, Li WJ, Tuan RS, Chang WH. Modulation of osteogenesis in human mesenchymal stem cells by specific pulsed electromagnetic field stimulation. J Orthop Res. 2009;27(9):1169-74.
22. Wessel Stratford E, Daffinrud J, Munthe E, Castro R, Waaler J, Krauss S, et al. The tankyrase-specific inhibitor JW74 affects cell cycle progression and induces apoptosis and differentiation in osteosarcoma cell lines. Cancer Med. 2014;3(1):36-46.
23. Azzarelli R, Pacary E, Garg R, Garcez P, van den Berg D, Riou P, et al. An antagonistic interaction between PlexinB2 and Rnd3 controls RhoA activity and cortical neuron migration. Nat Commun. 2014;5.
24. Thanyaphoo S, Kaewsrichan J. Synthesis and evaluation of novel glass ceramics as drug delivery systems in osteomyelitis. J Pharm Sci. 2012;101(8):2870-82.
25. Akiyama Y. TFSEARCH: Searching transcription factor binding sites. Available:http://www.cbrc.jp/research/db/TFSEARCH.html
26. Zhang X, Yang M, Lin L, Chen P, Ma K, Zhou C, et al. *Runx2* overexpression enhances osteoblastic differentiation and mineralization in adipose-derived stem cells *in vitro* and *in vivo*. Calcif Tissue Int. 2006;79(3):169-78.
27. Zhou X, Zhang Z, Feng JQ, Dusevich VM, Sinha K, Zhang H, et al. Multiple functions of Osterix are required for bone growth and homeostasis in postnatal mice. Proc Natl Acad Sci USA. 2010;107(29):12919-24.
28. Lu M, Amano S, Miyamoto K, Garland R, Keough K, Qin W, et al. Insulin-induced vascular endothelial growth factor expression in retina. Invest Ophthalmol Vis Sci. 1999;40(13):3281-6.
29. Hie M, Iitsuka N, Otsuka T, Tsukamoto I. Insulin-dependent diabetes mellitus decreases osteoblastogenesis associated with the inhibition of Wnt signaling through increased expression of Sost and Dkk1 and inhibition of Akt activation. Int J Mol Med. 2011;28(3):455-62.
30. Neve A, Corrado A, Cantatore F. Osteocytes: Central conductors of bone biology in normal and pathological conditions. Acta Physiol. 2012;204(3):317-30.
31. Chen J, Long F. β-catenin promotes bone formation and suppresses bone resorption in postnatal growing mice. J Bone Miner Res. 2013;28(5):1160-9.
32. Glass DA, Bialek P, Ahn JD, Starbuck M, Patel MS, Clevers H, et al. Canonical Wnt signaling in differentiated osteoblasts controls osteoclast differentiation. Dev Cell. 2005;8(5):751-64.
33. Conti F, Wolosinska D, Pugliese G. Diabetes and bone fragility: A dangerous liaison. Aging Clin Exp Res. 2013;25(1): 39-41.
34. Yavropoulou MP, Yovos JG. The role of the Wnt signaling pathway in osteoblast commitment and differentiation. Hormones. 2007;6(4):279.
35. Gatti D, Viapiana O, Fracassi E, Idolazzi L, Dartizio C, Povino MR, et al. Sclerostin and DKK1 in postmenopausal osteoporosis treated with denosumab. J Bone Miner Res. 2012;27(11):2259-63.
36. Etheridge SL, Spencer GJ, Heath DJ, Genever PG. Expression profiling and functional analysis of wnt signaling mechanisms in mesenchymal stem cells. Stem cells. 2004;22(5):849-60.
37. Tandon M, Gokul K, Ali SA, Chen Z, Lian J, Stein GS, et al. *Runx2* mediates epigenetic silencing of the bone morphogenetic protein-3B (BMP-3B/GDF10) in lung cancer cells. Mol cancer. 2012;11(1):1.
38. Byun MR, Kim AR, Hwang JH, Kim KM, Hwang ES, Hong JH. FGF2 stimulates osteogenic differentiation through ERK

induced TAZ expression. Bone. 2014;58: 72-80.
39. Lefebvre V, Dumitriu B, Penzo-Méndez A, Han Y, Pallavi B. Control of cell fate and differentiation by Sry-related high-mobility-group box (Sox) transcription factors. Int J Biochem Cell Biol. 2007;39(12):2195-214.
40. Long F. Building strong bones: Molecular regulation of the osteoblast lineage. Nat Rev Mol Cell Biol. 2012;13(1):27-38.
41. Lee KS, Kim HJ, Li QL, Chi XZ, Ueta C, Komori T, et al. *Runx2* is a common target of transforming growth factor β1 and bone morphogenetic protein 2, and cooperation between *runx2* and Smad5 induces osteoblast-specific gene expression in the pluripotent mesenchymal precursor cell line C2C12. Mol Cell Biol. 2000;20(23): 8783-92.
42. Drissi H, Luc Q, Shakoori R, Chuva De Sousa Lopes S, Choi JY, Terry A, et al. Transcriptional autoregulation of the bone related CBFA1/RUNX2 gene. J Cell Physiol. 2000;184(3):341-50.

Peer-review history:
The peer review history for this paper can be accessed here:
http://sciencedomain.org/review-history/22026